

Critical Thickness in Dewetting Films

B. Du, Z. Yang, and O. K. C. Tsui *

Institute of Nano Science and Technology and Department of Physics, Hong Kong University of Science and Technology, Clear Water Bay, Kowloon, Hong Kong.

We study dewetting of thin polymer films with built-in topographical fluctuations produced by rubbing the film surface with a rayon cloth. By varying the density of imposed surface defects, we unambiguously distinguish spinodal dewetting, which dominates in liquid films thinner than a characteristic thickness = 13.3 nm, from heterogeneous nucleation in the thicker films. Invariance of this characteristic thickness upon more than a decade change in the defect density makes kinetic effect an unseemly origin. A crossover of the spinodal line provides a consistent picture. This interpretation, however, contends the current understanding of molecular interactions in apolar liquid films.

68.15.+e, 47.20.-k, 68.45.-v

arXiv:cond-mat/0110123v1 [cond-mat.soft] 6 Oct 2001

*To whom correspondence should be addressed. Electronic address: phtsui@ust.hk

A physical state is unstable if the curvature of its free energy, G with respect to the order parameter, h is negative. According to the mean-field theory of Cahn [1], such states may proceed to equilibrium via a spinodal mechanism that results in a spatial modulation of the order parameter. It can be shown that the mode with wavelength, $\lambda_m = (-4\pi^2\gamma/d^2G/dh^2)^{\frac{1}{2}}$ will grow the fastest, where γ is the rigidity of the system order parameter against deviations from homogeneity. Alternatively, the system may evolve to equilibrium by nucleation of heterogeneity at defect sites from within. For a long time, the distinction between these two mechanisms in the dewetting of liquid films from a non-wetting substrate has been the subject of many contentious debates [2–11].

In supported apolar liquid films, the non-retarded Lifshitz-van der Waals interactions render the unit area free energy the form $-A/12\pi h^2$ [12], where A is the Hamaker constant and h - the system order parameter - is the liquid film thickness. Therefore, thin liquid films wherein $A > 0$ will rupture spontaneously by spinodal growth of surface capillary waves, for which the fastest growing mode has the wavelength, $\lambda_m = (16\pi^3\gamma/A)^{\frac{1}{2}}h^2$ [7,13,14] (Here, γ is the surface tension of the liquid.) Previous experiments find that dewetting of liquid films proceed according to a generic sequence [2–9] beginning with a thickness modulation, often noted as holes, followed by the coarsening of the holes and formation of a polygon network, with the eventual breakup of the polygon network into droplets due to the Rayleigh instability [15]. While the latter processes are governed by hydrodynamics of dewetting and well understood [14–16], opinions are divided on the mechanism (i.e. spinodal or heterogeneous nucleation) underlying the crucial initial step. An h^{-2} dependence frequently found in the dewetting wavevector [4–7,10] has been taken as evidence for spinodal dewetting. However, Jacobs et al. [9] found the holes to have no positional correlation, thereby unlikely a result of spinodal surface undulations. In addition, the h^{-2} dependence apparent in the experimental characteristic wavevector has also been argued to resemble an exponential variation $\sim \exp(-h/L)$ ($L = \text{constant}$), fitting to be considered an evidence of heterogeneous nucleation from intrinsic defects. Furthermore, it was found in dewetting experiments of metal thin films [10] and evaporating volatile liquid films [11] that morphologies due to both kinds of mechanisms may sometimes coexist. This adds further complications to the attempt to make a clean distinction between the two destabilizing mechanisms using conventional approaches that rely on direct analysis of the dewetting patterns.

In this experiment, we used polystyrene (PS) spin-coated on silicon covered with an oxide layer as the model system, which is the most studied for this problem. We artificially introduce small height fluctuations, δh (≤ 1 nm) to the thin film samples by mechanically rubbing the sample surface with a rayon cloth before dewet-

ting initiates. For liquid films that dewet by nucleation, the characteristic length of the dewetting pattern depend on the density of surface fluctuations introduced. But for those films that dewet by a spinodal process, the characteristic length should remain unaffected [17]. Therefore, simply by comparing the dewetting morphologies with and without the rubbing-induced surface defects, one can unambiguously identify which of the two dewetting mechanisms dominates. Our results show that the final pattern of all dewet films is always dictated by *just one* mechanism. For the present system (PS/SiO₂/Si), it is found that spinodal dewetting dominates in the thinner films ($h < 13.3$ nm) whereas heterogeneous nucleation dominates in the thicker ones. Abruptness of the transition at $h = 13.3$ nm between the two mechanisms suggests that it is of a thermodynamic rather than kinetic nature. We attribute the transition to a crossover of the spinodal line, which however may present challenge to our understanding of molecular interactions for the present liquid film system. We will elaborate further on this point below. By examining the dewetting morphologies in different regions with respect to the critical thickness, we are able to make direct comparison between experiment and theoretical predictions [8] on dewetting pattern formation. Excellent agreement between theory and experiment is obtained. Our results thus resolve the controversy by showing that the two mechanisms are operative in different thickness regions separated by a transition.

The PS sample was purchased from Scientific Polymer Products (Ontario, NY). It has a molecular weight of 13.7K Da and polydispersity 1.1. The glass transition temperature was measured to be ~ 99 °C by differential scanning calorimetry. The substrate overlayer was prepared by wet oxidation: 4" diameter Si(100) wafers cleaned as described previously [18] were annealed at 1000 °C in a reaction chamber filled with water vapor (produced by a simultaneous injection of 5.6 L/min. H₂ and 4 L/min. O₂ into the chamber) for 9 mins. 40 sec. The thermal oxide was confirmed to be 106 nm thick by spectroscopic ellipsometry with better than 1 % uniformity. The oxidized wafers were then cut into square pieces of 1 × 1 cm², and cleaned [18] before coated with the polymer. Both the substrate cleaning and polymer coating were carried out in a clean room. Before use, the polymer films were annealed at 100 °C under vacuum (10⁻² torr) for 5 h to remove the residue solvent. No sign of dewetting was detectable in the samples after annealing. To produce the artificial topographical fluctuations, a piece of rayon cloth loaded with a normal pressure of 10 g/cm² was rubbed against the film surface at a constant speed = 1 cm/s by an electric motor. The density of surface defects was varied by changing the number of rubs applied to the films. Sample topography was characterized by a Seiko Instruments (Chiba, Japan) SPA-300HV atomic force microscope (AFM). Fig. 1 shows the

Fourier spectra for the surface topography of five freshly rubbed PS films that had been rubbed with different number of times ($N = 3$ to 15). These spectra were obtained by radial averaging the two-dimensional (2D) fast Fourier transformation (FFT) of AFM topographical images ($5 \times 5 \mu\text{m}^2$) obtained from the samples. As seen, all spectra look alike. Except for a gentle, but obvious rise towards $q = 0$ and a small peak at $q = 120 \mu\text{m}^{-1}$, the spectra are overall speaking rather flat. From the FFT images (for example, left inset of Fig. 1), one can see that the spectra are dominated by anisotropic topographies parallel to the rubbing direction. We found that the film roughness could be fitted to $(0.26^2 + 0.16^2 N)^{\frac{1}{2}}$ (nm) (solid line in the right inset of Fig. 1). All these characterizations about the topography of the rubbed films suggest that addition of height fluctuations in the films by individual rubs are independent events. It thus follows that the density of rubbing-induced surface defects should increase linearly with N .

Dewetting experiments were carried out in air. The films were annealed at 180°C for 10 to 60 mins. We deduce the characteristic wavevector, q^* of the final dewetting patterns from the peak of their radial averaged Fourier spectra. When the initial holes do not coalesce to form a network of polygons before break up into droplets, which has been found in thinner films where $h < 13.3$ nm, $(q^*)^2$ will be $\sim N_d$, the areal density of the final liquid droplets [4]. For the thicker ones, $(q^*)^2$ is $\sim N_p$, the areal density of the polygons [5–7]. Fig. 2 depicts q^* vs. h for samples rubbed by different number of times ($N = 0$ to 10) in a 3D plot. As seen, the data are divided into two groups at $h = 13.3$ nm: Below 13.3 nm, q^* is independent of N ; but above, it increases with increasing N . This result unambiguously evidences that samples with $h < 13.3$ nm rupture by a spinodal mechanism whereas those with $h > 13.3$ nm rupture by nucleation of holes. We note that $q^*(h)$ of the unrubbed films fits quite well to $\sim h^{(-2.1 \pm 0.05)}$ for $h < 13.3$ nm, and $\sim h^{(-2.5 \pm 0.1)}$ for $h > 13.3$ nm (solid lines in Fig. 2). The fact that the latter is not notably different from the h^{-2} dependence could have been easily mistaken as the signature of spinodal dewetting. We have model-fit the data to an exponential function (data not shown) and obtained similar good fits as Jacobs et al. found [9]. This finding confirms the earlier suggestion by these authors that the $q^* \sim h^2$ scaling characteristic is insufficient for the distinction between spinodal and nucleation dewetting.

We now examine evolution of the dewetting morphology of unrubbed PS films in different thickness regimes about the threshold at $h = 13.3$ nm. Fig. 3 shows AFM topographical images obtained from a 6.8 nm thick PS film upon quenching at different annealing times from 3 sec. to 23 min. at 145°C . As seen, uniformly sized holes first appeared after 10 sec., which enlarged and developed into a bicontinuous structure after 7 mins. In Fig. 4, we contrast evolution of the rupturing morphology

at 145°C of PS films near the threshold: one just below at $h = 12.8$ nm and one just above at $h = 13.8$ nm. For the $h = 12.8$ nm thick PS film (Fig. 4(a)), non-uniformly sized holes were first found scattering randomly across the sample after 4 mins. They grew in size, and more holes emerged with time. Until ~ 28 mins. the holes filled up the entire area of the film whereupon the thin ribbons connecting the holes broke up into droplets. The $h = 13.8$ nm thick PS film, though differ in thickness from the $h = 12.8$ nm one by only 1 nm, undertook a drastically different pathway (Fig. 4(b)). As seen, randomly distributed holes also appeared in the first few minutes, but their size and number never grew large enough to cover up the entire film at similar times it had taken the $h = 12.8$ nm thick film. Instead, only bigger holes with a much lower areal coverage could be seen growing and emerging, which after a much longer time of ~ 100 mins., finally touch each other and coalesced into polygons before the thin ribbons connecting the polygons broke up into droplets.

With illustrations of Figs. 3 and 4, we may summarize on what kinds of conformation can be formed in the early stage of spinodal dewetting of supported liquid films. Basically, both a bicontinuous structure (Fig. 3) and distribution of circular holes (Fig. 4(a)) can form in the initial stage of a spinodal process. Our results show that the bicontinuous structure is formed only in samples in the deep spinodal region whereas circular holes are formed in samples closer to the spinodal line, consistent with the 3D nonlinear calculations of Sharma et al. [8]. It is, however, noteworthy that the linear theory [1] will have predicted only the formation of a bicontinuous structure. Our result, therefore, clearly demonstrates inadequacy of the linear theory in accounting for the spinodal process. Another point to note is that the circular holes formed generally do not have positional correlations (see Fig. 4(a)) although the characteristic q^* is still the same as the one predicted by the linear theory [1,13,14], which is again in consistency with Ref. [8].

It remains to understand what causes the transition between different dewetting mechanisms near $h = 13.3$ nm. Similar transition has also been observed in previous experiments [3,5]. Meredith et al. attributed the transition to a crossover between spinodal and nucleation process due to kinetic dominance of the latter over the former at large h [19]. We note that the critical thickness remains unchanged even when the density of rubbing-induced defects is varied by more than an order of magnitude. Kinetic effects will require that the critical thickness should change by more than a factor $\sim 10^{\frac{1}{5}} (= 1.58)$ [19], which is obviously not evident in the data of Fig. 2. Therefore, it is most probable that the transition represents a crossover of the spinodal line. This interpretation, however, necessitates that the free energy has an inflection point at $h \approx 13.3$ nm. Using the more precise form of the free energy proposed in Ref. [7] to take into account that

the present system, is a PS/SiO₂/Si tri-layer rather than a simple bilayer one for which the $G \sim A/h^2$ relation is derived, one will obtain a prediction for the position of the spinodal line to be at $h \geq \delta = 106$ nm, the thickness of SiO₂ in this experiment. At present, the reason for the discrepancy between the predicted and the observed transition at $h = 13.3$ nm is not entirely clear. It is though apparent that retardation effects may no longer be negligible for the Lifshitz-van der Waals interactions across the SiO₂ layer since $\delta \approx 100$ nm is quite large in this study [12]. However, retardation effects will more likely worsen the discrepancy between the predicted and the experimental critical thickness. Studies are currently being carried out to understand how the SiO₂ inter-layer thickness affects the position of the critical thickness. It is hoped that with the insight thus gained about the form of van der Waals interactions in a tri-layer system, stability of thin liquid films can be premeditated.

We thank R. Seemann, K. Jacobs and S. Herminghaus for sending us their manuscript prior to publication. Critical reading of this manuscript by P. Sheng is gratefully acknowledged. This work is supported by the Institute of Nano Science and Technology, HKUST.

-
- [1] J. W. Cahn, J. Chem. Phys. **42**, 93 (1965).
 [2] G. Reiter, A. Sharma, A. Casoli, M.-O. David, R. Khanna, P. Auroy, Langmuir **15**, 2551 (1999).
 [3] R. Xie, A. Karim, J. F. Douglas, C. C. Han, R. A. Weiss, Phys. Rev. Lett. **81**, 1251 (1998).
 [4] G. Reiter, A. Sharma, A. Casoli, M.-O. David, R. Khanna, P. Auroy, Europhys. Lett. **46**, 512 (1999).
 [5] J. C. Meredith, A. P. Smith, A. Karim, E. J. Amis, Macromolecules **33**, 9747 (2000).
 [6] G. Reiter, Phys. Rev. Lett. **68**, 75 (1992).
 [7] A. Sharma, G. Reiter, J. Colloid Interface Sci. **178**, 383 (1996).
 [8] A. Sharma, R. Khanna, Phys. Rev. Lett. **81**, 3463 (1998).
 [9] K. Jacobs, S. Herminghaus, K. R. Mecke, Langmuir, **14**, 965 (1998).
 [10] J. Bischof, D. Scherer, S. Herminghaus, P. Leiderer, Phys. Rev. Lett. **77**, 1536 (1996).
 [11] U. Thiele, M. Mertig, W. Pompe, Phys. Rev. Lett. **80**, 2869 (1998).
 [12] J. Israelachvili, *Intermolecular and Surface Forces*, 2nd Ed., Academic Press, London, 1991.
 [13] A. Vrij, J. Th. G. Overbeek, J. Am. Chem. Soc., **90**, 3074 (1968)
 [14] F. Brochard-Wyart, J. Daillant, Can. J. Phys., **68**, 1084 (1990).
 [15] Lord Rayleigh, Proc. London Math. Soc. **10**, 4 (1878).
 [16] C. Redon, F. Brochard-Wyart, F. Rondelez, Phys. Rev. Lett. **66**, 715 (1991).
 [17] In O. C. Tsang, O. K. C. Tsui, Z. Yang, Phys. Rev. E,

63, 061603 (2001), it was found that the rubbing-induced strain in PS films is fully relaxed within seconds upon annealing above the T_g of the polymer. Therefore, any perturbation due to the strain on G is relaxed to zero well within the spinodal rupture time, thus cannot play a major role in the film rupture process.

- [18] X. P. Wang, X. Xiao, O. K. C. Tsui, Macromolecules, **34**, 4180 (2001).
 [19] The growth rate for the size of nucleated holes $\sim \gamma\theta^3/\eta$ [14] (where θ is the equilibrium contact angle between the liquid and the substrate surface) is relatively independent of h , but the amplitude growth rate of surface undulations, $R_m \sim h^{-5}$ [5,13,14] decreases rapidly as h increases.

FIG. 1. Fourier spectra of surface topography of PS films rubbed with different number of times. Left inset shows FFT image obtained from an AFM topographical image of a PS film that was rubbed 10 times. Right inset shows the roughness of rubbed PS films vs. number of rubs. Filled circles are data. Solid line is the model fit (see text).

FIG. 2. 3D plot of the characteristic wavevector, q vs. h for PS films rubbed by different number of times from 0 to 10. Solid lines are fits to a power law. Thin dotted lines are contour lines at $h = 7, 13.3$ and 30 nm.

FIG. 3. AFM topographical images of a 6.8 nm thick PS film taken after quenching at different annealing times from 10 sec. to 23 mins. at 145°C.

FIG. 4. Comparison between dewetting morphology of (a) 12.8 nm and (b) 13.8 nm thick PS films at 145°C. All pictures are AFM topographical images except the last two in (b), which are optical micrographs.

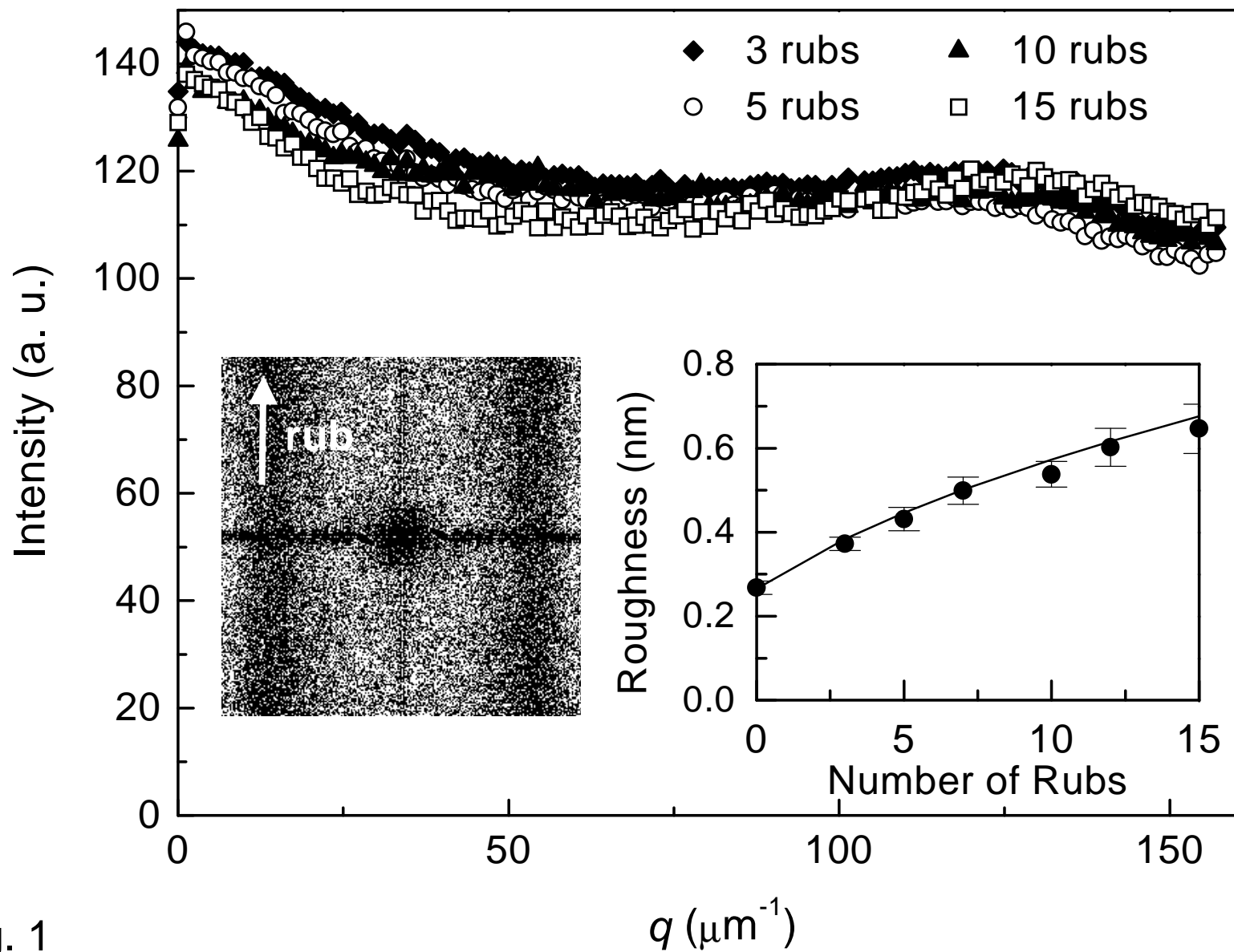


Fig. 1

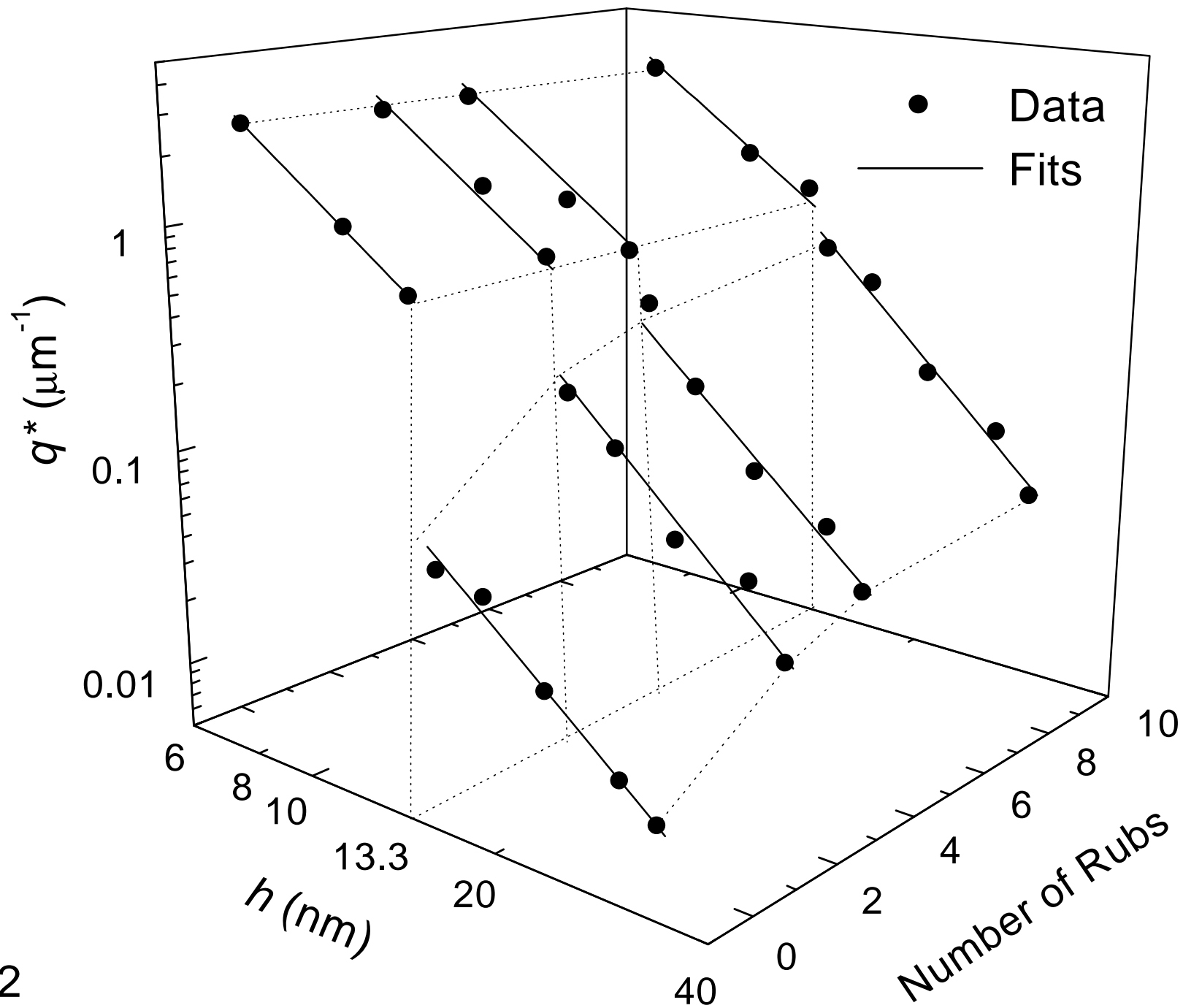


Fig. 2

This figure "Fig3.JPG" is available in "JPG" format from:

<http://arxiv.org/ps/cond-mat/0110123v1>

This figure "Fig4a.JPG" is available in "JPG" format from:

<http://arxiv.org/ps/cond-mat/0110123v1>

This figure "Fig4b.JPG" is available in "JPG" format from:

<http://arxiv.org/ps/cond-mat/0110123v1>